

Metabolomics and biochemical insights on the regulation of aging-related diabetes by a low-molecular-weight polysaccharide from green microalga *Chlorella pyrenoidosa*

Yinghui Qiu^{a,1}, Xiaoxiang Gao^{a,1}, Ruoxin Chen^a, Suyue Lu^a, Xuzhi Wan^a, Mohamed A. Farag^d, Chao Zhao^{a,b,c,*}

^a College of Food Science, Fujian Agriculture and Forestry University, Fuzhou 350002, China

^b Engineering Research Centre of Fujian-Taiwan Special Marine Food Processing and Nutrition, Ministry of Education, Fuzhou 350002, China

^c Key Laboratory of Marine Biotechnology of Fujian Province, Institute of Oceanology, Fujian Agriculture and Forestry University, Fuzhou 350002, China

^d Department of Pharmacognosy, Faculty of Pharmacy, Cairo University, Cairo 11562, Egypt

ARTICLE INFO

Keywords:

Chlorella pyrenoidosa polysaccharide
Metabolomics
Type 2 diabetes
Antioxidant
Phenylpyruvic acid

ABSTRACT

Globally, aging and diabetes are considered prevalent threats to human health. *Chlorella pyrenoidosa* polysaccharide (CPP) is a natural active ingredient with multiple health benefits including antioxidant and hypolipidemic activities. In this study, the aging-related diabetic (AD) mice model was established to investigate the underlying hypoglycemic and antioxidant mechanisms of CPP. It improved superoxide dismutase, catalase (CAT), glutathione peroxidase (GSH-px), and malondialdehyde activities in liver and insulin secretion. CAT and GSH-px activity in the brain increased after CPP administration. In addition, through histopathological examinations, it was evident that injuries in the liver, brain, jejunum, and pancreas were restored by CPP. This restoration was likely mediated via the activation of glucagon-like peptide-1 receptor/FOXO-1 (forkhead box O1) pathway concurrent with the inhibition of interleukin-6 receptor/FOXO-1 pathway. Furthermore, metabolomics and correlation analysis revealed that CPP possibly relieved AD through changes in insulin levels and declined oxidative stress as regulated by phenylpyruvic acid. These findings suggested that CPP exerted antioxidant and hypoglycemic roles in an AD mice model, thereby providing a sound scientific foundation for further development and utilization of CPP.

Introduction

Type II diabetes (T2D) is a common chronic disease. It accounts for 90%–95% cases of diabetes mellitus, a relatively common metabolic syndrome which is accompanied by certain complex complications including generalized brain atrophy, greater high-intensity lesion volumes, hippocampal, and amygdala atrophy (Kazeem et al., 2021; Lee et al., 2012; Zhao et al., 2020). Typically, this disease is known to occur in older adults, and the number of aging-related diabetic (AD) patients progressively increases owing to aging of the islet β -cells (Atella et al., 2019; Fuster et al., 2020). One of the most common causes of mortality in older adults is diabetes (Longo et al., 2019). However, aging and T2D have a complementary relationship, in which T2D could accelerate aging. High blood sugar causes the mitochondrial electron transport

chain to produce large amounts of superoxide and nitric oxide, which subsequently further accelerates aging (Giacco and Brownlee, 2010). Therefore, it is imperative to establish AD model and examine the effects of AD on the brain.

D-(+)-Galactose (D-gal) is a common inducer for aging and is detected at high levels in the brain of older adults (Wei et al., 2005). Streptozotocin (STZ), a nitrosourea with DNA alkylating properties, is widely used in diabetes models and is known to damage β -cells. D-gal and STZ administration results in oxidative stress by increasing the production of reactive oxygen species (ROS) and prolonging the injury recovery owing to high brain glucose levels (Aydin et al., 2016; Metwally et al., 2018). Therefore, a combination of both reagents could be used to induce AD. Forkhead box O1 (FOXO-1) plays an important role in mediating the effect of insulin on hepatic metabolism, and increased

* Corresponding author at: College of Food Science, Fujian Agriculture and Forestry University, Fuzhou 350002, China.

E-mail address: zhchao@live.cn (C. Zhao).

¹ Yinghui Qiu and Xiaoxiang Gao contributed equally to this study.

FOXO-1 activity was found to be associated with a reduction in the of insulin to regulate hepatic glucose level (Benchoula et al., 2021). FOXO-1 shows decreased levels with aging and thereby leads to the development of diabetes owing to the fact that FOXO-1 represses the production of glucokinase to suppress the glucose production (Benchoula et al., 2021). FOXO-1 is associated with the regulation of zona occludens-1 (ZO-1) and matrix metalloproteinase-2 (MMP-2) that play an important role in the protection of blood–brain barrier and B-cell lymphoma-6 (BCL-6) inhibition, a process that inhibits cell apoptosis (Glauser and Schlegel, 2009; Huang and Li, 2014). Typically, aging is accompanied by inflammation, which may lead to the activation of interleukin-6 receptor (IL-6R) and the inactivation of glucagon-like peptide-1 receptor (GLP-1R), thereby decreasing FOXO-1 levels to induce cell death (Wang et al., 2009; Kim et al., 2015). Assessing changes in the blood–brain barrier, oxidative stress, and inflammation in the brain and examining the associated molecular mechanism is of paramount importance to identify the target substance to prevent AD.

Chlorella pyrenoidosa is a unicellular green alga that is rich in macronutrients such as proteins, polysaccharides, lipids, and micronutrients (vitamins). The polysaccharides derived from *C. pyrenoidosa* account for several of its pharmacological activities, such as antioxidant, antitumor, antihypertensive, anti-inflammatory, and anti-diabetes (Wan et al., 2019). *C. pyrenoidosa* polysaccharides (CPP) with a molecular weight of > 3000 Da reportedly improved antioxidant activities in *Caenorhabditis elegans* and exerted hypolipidemic effects in rats (Wan et al., 2019; Wan et al., 2021). The detailed characterization of green microalga *C. pyrenoidosa* polysaccharide included in the present study has been previously published (Wan et al., 2021). However, the effects of CPP on AD rat models remain unknown and the underlying mechanism requires further elucidation. In the present study, AD mice model was used to assess the functions of CPP and action mechanisms using metabolomics and molecular biology techniques to monitor changes in endogenous metabolites in the brain and changes in gene expression levels. This study aimed to provide novel evidence for the regulation of AD using CPP and to improve the current understanding of AD progression at the metabolite level.

2. Material and methods

2.1. Preparation of CPP

C. pyrenoidosa powder (100 g), purchased from Fuqing King Dnarmsa Spirulina Co., Ltd (Fuzhou, China), was dissolved in distilled water (4000 mL) using supersonic extraction with 45 kHz at 60 °C for 2 h. After filtration, the solution was centrifuged at 5000 rpm for 10 min, following which the supernatant was concentrated and mixed with 4 × ethanol at 4 °C overnight. The ethanol was removed and the precipitate was collected for deproteinization. Neutral protease with 50,000 units/mL enzyme activity was then used to remove the protein before boiling the mixture for 10 min to inactivate the enzyme. Subsequently, 8–14 kDa Cutoff dialysis membranes were employed to collect CPP. In the next stage, 0.1 mol/L sulfuric acid was used to degrade CPP, which was then neutralized using NaOH. This solution was condensed and mixed with an equal volume of ethanol before centrifugation of 5000 rpm for 10 min. The supernatant was then collected for freeze drying. CPP (molecular weight > 3 kDa) was collected using 3 kDa cutoff dialysis membranes for further analysis and freeze drying for animal experiments.

2.2. Animals experiment & study design

Fifty male Kunming mice (SPF grade; age, 6 weeks; body weight, 20–27 g) were purchased from Wu's Animal Laboratory Center Co., Ltd. (Fuzhou, China). The mice were raised under standard conditions (25–27 °C, 55% relative humidity, and 12 h daylight cycle) with the rodent chow diet. After a week of adaptation, mice were randomly

categorized into five groups as follows: 10 mice were selected into normal group fed with normal diet (Normal), and the remaining mice were fed with high-glucose-high-fat diet (15% lard, 15% sucrose, 1% cholesterol, 10% yolk, 0.2% sodium deoxycholate, and 58.8% standard chow) until the end for consistency conditions in the whole experiment. The mice fed with high-glucose-high-fat diet were administered 45 mg/kg of D-gal prepared with saline every day for 1 month. After a month, diabetes was induced via STZ (50 mg/kg) administration twice a week (Ouyang et al., 2022). The blood sample of overnight fasted mice were then collected from the tail vein. The HGM-114 glucometer (Omron, China) was used to determine blood glucose level. Mice with glucose levels above 11.1 mmol/L were regarded as diabetic mice (Sivaraman et al., 2013). Mice fed with D-gal and STZ were randomly divided into four groups as follows: **A.** mice were administered saline (AD); **B.** mice were treated with 90 mg/kg metformin dissolved in saline (DMBG) **C** & **D.** mice received 150 mg/kg of CPP and 300 mg/kg of CPP dissolved in saline (CPPL and CPPH). At the end of the animal experiments, the mice were anaesthetized with 1% pentobarbital sodium and then sacrificed using cervical dislocation after fasting for 12 h. The pancreas, brain tissue, jejunum, epididymis fat, and liver were harvested and stored at –80 °C for biochemical and histopathological analyses as well as metabolomics analysis. The body weight of all animals was recorded before the treatment and at the end of experiment. All animal experiments and protocols were in accordance with the most humane care and use of animals and Institutional Animal Ethics of College of Food Science, Fujian Agriculture and Forestry University (FS-2019–006).

2.3. Assessment of enzymatic capacity and MDA

We mixed 100 mg lyophilized liver and brain with 0.9% saline to prepare the tissue homogenate. After centrifugation at 5000 rpm for 10 min at 4 °C, the supernatant was collected for the analysis of superoxide dismutase (SOD), catalase (CAT), and glutathione peroxidase (GSH-px) as well as malondialdehyde (MDA) according to assay kits by vendor (Jiancheng Biotechnology, Nanjing, China).

2.4. Glucose tolerance test and insulin assay

After fasting for 12 h, the oral glucose tolerance test (OGTT) was performed at 0, 0.5, 1, and 2 h. The formula of oral glucose tolerance area (AUC) is as follows:

$$AUC = 0.25 \times (G_0 \text{ h} + G_{0.5\text{h}}) + 0.25 \times (G_{0.5\text{h}} + G_{1 \text{h}}) + 0.5 \times (G_{1 \text{h}} + G_{2 \text{h}}).$$

The serum samples were separated after being centrifuged at 3000 rpm/min for 10 min at 4 °C and stored at –80 °C. The level of serum insulin was measured using an ELISA technique kit (Shengkeboyuan Biotechnology, Beijing, China).

2.5. Histopathological and immunohistochemical (IHC) examination

The tissue samples including, brain, jejunum, liver, and pancreas, were cleaned with saline and fixed in 10% buffered formalin, embedded in paraffin wax, and then cut into 5-μm thick slices. The hematoxylin and eosin were used to evaluate the histopathological changes in the tissues. For IHC analysis, the slices were deparaffinized in xylol and rehydrated using ethyl alcohol. After antigen retrieval in citrate buffer (pH 6.0), the sections were treated with 0.03% hydrogen peroxide to block the endogenous peroxidase. The samples were then incubated with primary antibodies, including GLP-1R, FOXO-1, BCL-6, IL-6R, and MMP-2, at 4 °C overnight. All antibodies were purchased from Sangon Biotechn (Sangon Biotechn, Shanghai, China). After incubation with the associated secondary antibody, the sections were stained with diaminobenzidine and re-stained with hematoxylin. The histopathological changes and protein expression of these samples were observed using a fluorescent microscope (Scope.A1, Zeiss, Oberkochen, Germany).

2.6. Real-time quantitative PCR (RT-qPCR) analysis

To investigate the relative mRNA expression, TRIzol® was used to isolate total RNA from mouse brain (100 mg). TAKARA cDNA synthesis kit (TAKARA, Japan) was employed for reverse transcription according to manufacturer protocol. After reverse transcription, mRNA expression was detected using SYBR Premix Ex Taq II kit (TAKARA, Japan) by ABI7300 (Applied Biosystem, CA, US). The program was used according to the manufacturer's instructions (TAKARA, Japan). The $2^{-\Delta\Delta Ct}$ method was used to calculate relative mRNA expression. Primers are listed in Table S1 and β -actin is regarded as the reference gene.

2.7. LC/MS analysis

Brain tissue (5 mg) of mice in CPPH group was homogenized with MeOH: H₂O (4:1, v/v) and 10 μ L 100 μ g/mL specific marker CA-d4 added as an internal standard. After centrifugation for 5 min at 13000 rpm, 400 μ L supernatant was mixed with the MeOH:H₂O. The dried extract was obtained using a nitrogen evaporator and then dissolved in 100 μ L ultrapure water. After centrifugation for 5 min, the supernatant was used for metabolite profiling using liquid chromatography (Ultimate 3000, Thermo Fisher Scientific, USA) coupled with negative electrospray ionization (NDK200-2 N, Miou, China). Quadrupole-time-of-flight (Q Exactive, Thermo Fisher Scientific, USA). SIMCA-P 14.1 (Umetrics, Umea, Sweden) was used to visualize intergroup changes in metabolites. Principal component analysis (PCA), projection to latent structure discriminant analysis (OPLS-DA), and variable importance in the projection (VIP) plot were employed to observe the intergroup differences and detect differential metabolite markers, with VIP values above 1.5 regarded as key tools to identify potential biomarkers. These biomarkers were identified by KEGG (<https://www.kegg.jp/>) and HMDB (<https://www.hmdb.ca/>)

databases. The metabAnalyst 4.0 (<https://www.metaboanalyst.ca/>) was used to analyze the key metabolic pathway treated by CPP.

2.8. Statistical analysis

All study outcomes were expressed as mean \pm standard deviation involving at least three independent experiments. Statistical analyses were conducted with one-way ANOVA and Student's *t*-test using Origin 2020 software (OriginLab, Massachusetts, USA). *P* value of < 0.05 indicated statistical significance.

3. Results and discussion

3.1. Effect of CPP on body and tissue weight of AD mice

To investigate the potential effect of CPP on AD mice, body-weight changes were examined (Fig. 1a). The average weight of normal mouse and drug-induced mice before treatment appeared to show significant differences ($p < 0.05$). This could be attributable to the effects of STZ and D-gal; furthermore, mice weight loss has been considered as one of the most common indicators associated with aging and diabetes (Suthagar et al., 2009; Yuan et al., 2020). After treatment with CPP and DMBG, mice body weight appeared to recover significantly ($p < 0.05$). Additionally, the D-gal and STZ groups showed increments in kidney weight ($p < 0.05$). However, this increase in weight recovered in the CPP and DMBG groups ($p < 0.05$) (Fig. 1b). STZ caused renal hypertrophy, increased glomerular volume, mesangial proliferation and accumulation of glomerular extracellular matrix, which may result in increased kidney weight (Zafar and Hassan Naqvi, 2010). In addition, mice in AD group gained more liver weight after drug induction, whereas CPPL, CPPH, and DMBG mice showed significant decrease in liver weight (Fig. 1c) ($p < 0.01$). Fromenty et al. reported that increased liver weight and fat

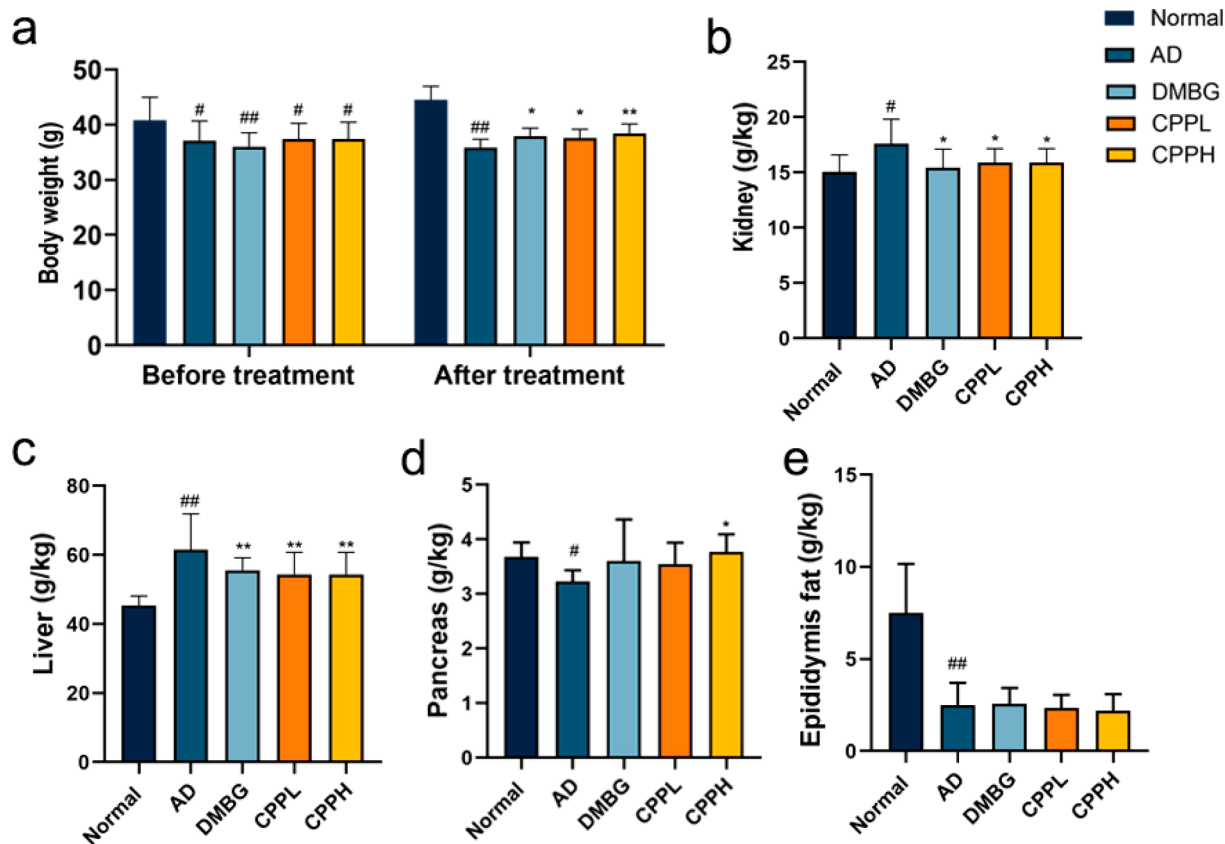


Fig. 1. Effects of CPP on the weight and viscera index of AD mice. (a) Bodyweight, (b) kidney weight, (c) liver weight, (d) pancreas weight, and (e) the weight of epididymis fat. Data are the mean \pm SD ($n = 10$). * $p < 0.05$, ** $p < 0.01$ vs. AD mice; # $p < 0.05$, ## $p < 0.01$ vs. normal mice.

accumulation occur in diabetic mice (Fromenty et al., 2009). Mice in the AD group showed a significant decrease in pancreas weight ($p < 0.05$), which could be attributable to the oxidative alterations induced by D-gal and STZ through the destruction of and the decline in the number of pancreatic islets (Samaha et al., 2019). Notably, 200 mg/mL CPP reduced the weight of pancreas ($p < 0.05$), whereas DMBG had no significant effect (Fig. 1d). Epididymal fat weight significantly decreased following STZ administration (Agunloye and Oboh, 2022; Huang et al., 2020) ($p < 0.01$). Weight of the epididymis fat in the normal group was significantly higher than that in the other four groups ($p < 0.01$). CPP and DMBG did not reverse the condition, indicating the CPP and DMBG barely inhibited the alleviation of epididymal fat (Fig. 1e). These results demonstrated that CPP administration helped in the recovery of kidney, liver, and pancreas injuries and improved body weight; however, it did not have any significant impact on epididymal fat.

3.2. Effect of CPP on glucose uptake in AD mice using OGTT

We examined the potential hypoglycemic effect of CPP on hyperglycemic activity by using OGTT to evaluate glycemic regulation and insulin tolerance (Fig. 2c & 2b). After glucose administration, the high

level of fasting blood glucose was detected in CPPL. This was owing to the fact that CPPL is insufficient to effectively control postprandial blood glucose at normal levels, or lead to nocturnal hypoglycemia and then lead to increase in hyperglycemic hormones in the morning (Bolli et al., 1984; Lin et al., 2021). Blood glucose peaked at 30 min in the AD group, reaching 30.6 ± 5.4 mmol/L, and then decreased to 29.72 ± 2.50 mmol/L at 120 min. However, the maximum glucose level in the CPP (200 mg/kg)-treated mice was 30.38 ± 4.27 mmol/L at 30 min, which was nearly identical to that in the AD group, and decreased to 20.06 ± 3.27 mmol/L at 120 min, thereby indicating a significant increase in glucose uptake ($p < 0.01$). Additionally, AD group showed an increase in AUC ($p < 0.01$), whereas DMBG and CPP significantly reduced the area under the curve ($p < 0.05$). STZ could damage pancreatic β cells and induce pancreatic β cells apoptosis, which leads to the decrease in insulin level and systemic immune system disorders (Metwally et al., 2018). In contrast, DMBG, CPPL, and CPPH supplementations significantly reversed the decreased amounts of insulin, compared with AD group (Fig. 2a) ($p < 0.01$). These results indicated that CPP and DMBG could improve the metabolism of glucose and protect islet β cells, thereby maintaining the production of insulin. Similar to the present study, previous studies reported that CPP could improve the regulation

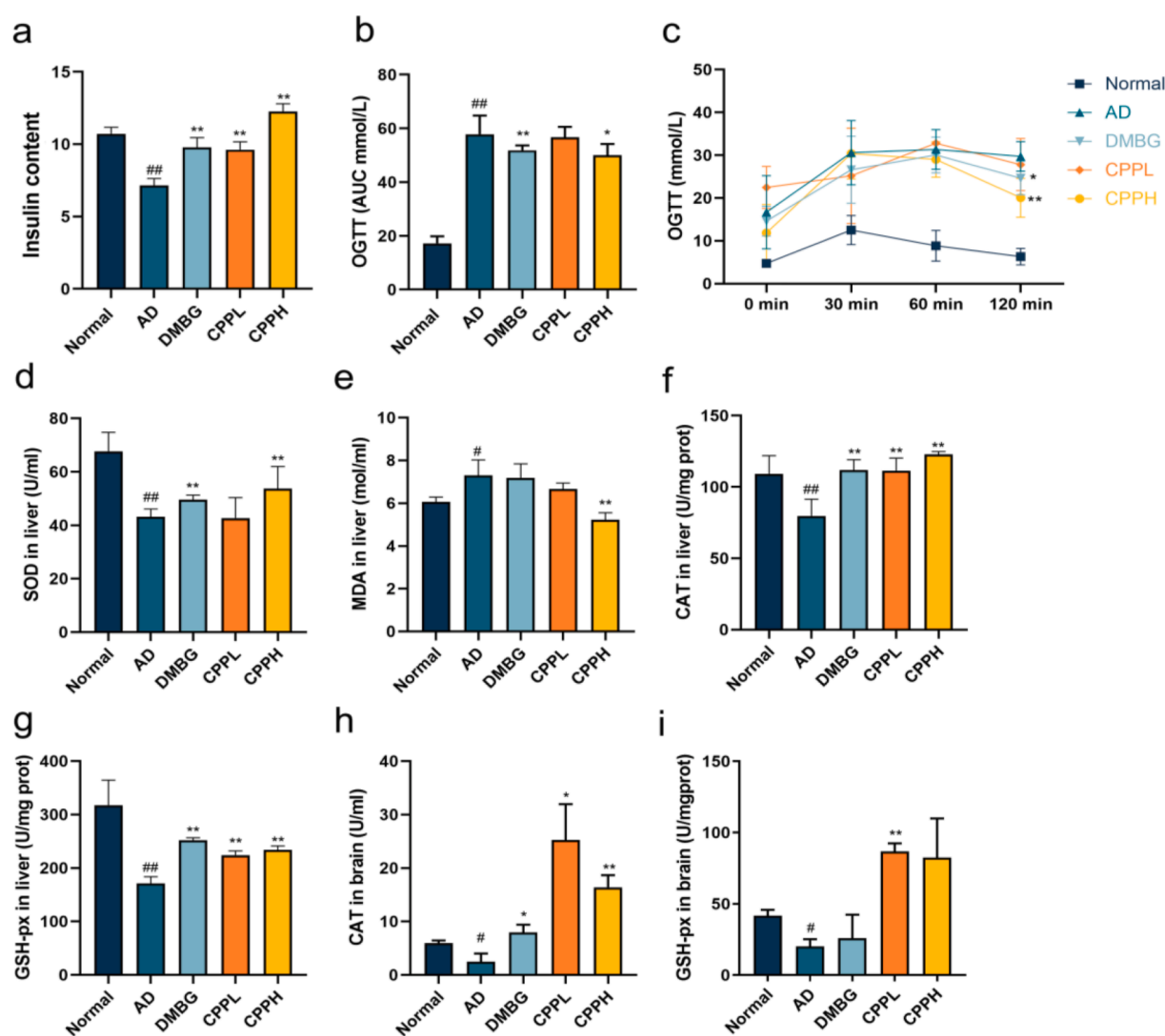


Fig. 2. Effect of CPP on the regulation of blood level and oxidative stress in AD mice. (a) CPP promoted insulin content after the induction of D-gal and STZ. (b & c) An oral glucose tolerance test was performed with fasted mice. The level of oxidative stress was evaluated by (d) SOD level in liver, (e) MDA content in liver, (f) CAT level in liver, and (g) GSH-px level in liver, as well as (h) CAT level in brain and (i) GSH-px level in brain. Values represent the mean \pm SD ($n = 7$). * $p < 0.05$, ** $p < 0.01$ vs. AD mice. # $p < 0.05$, ## $p < 0.01$ vs. normal mice.

of glucose metabolism in mice induced by STZ (Kim, 2018).

3.3. Effect of CPP on antioxidative enzyme levels and MDA in liver and brain

STZ accompanied with high-glucose-high-fat diet and D-gal both led to increased production of reactive oxygen species and oxidative stress (Aydn et al., 2016; Metwally et al., 2018). The levels of MDA, SOD, CAT, and GSH-px in liver were measured to investigate the therapeutic function of CPP in AD mice (Fig. 2d-g). Compared with normal animal group, D-gal and STZ both induced an increase in SOD activity in liver. CPP treatment led to a significant increase in SOD activity compared with AD group ($p < 0.01$). After induction, MDA level in AD group increased remarkably compared with normal group ($p < 0.05$), whereas CPPH animal group showed a significant reduction ($p < 0.01$). Liver CAT activity in AD group was obviously lower than normal group ($p < 0.01$). The CAT activity of CPPL and CPPH group as well as DMBG group increased significantly, compared with AD group ($p < 0.01$). Changes in liver GSH-px activity showed the same trend. CPP treatment significantly increased liver GSH-px level in comparison with AD group ($p < 0.01$). Interestingly, DMBG significantly increased GSH-px in the liver but not in the brain ($p < 0.01$). Other reports demonstrated that oral DMBG administration for 6 weeks did not significantly increase GSH level in the brain until 10 weeks (Oboh et al., 2018). These results suggested that CPP improved oxidative stress, thereby modulating organ aging. Similarly, other studies have demonstrated that pretreatment with CPP considerably diminished SOD and MDA levels in *Caenorhabditis elegans* (Wan et al., 2021).

Furthermore, the effects of CPP on brain oxidative stress markers were assessed (Fig. 2h & 2i). The brain GSH-px activity significantly decreased in the AD group ($p < 0.05$), whereas CPPL treatment consequently increased GSH-px production ($p < 0.01$). The AD group showed decreased CAT activity in comparison with the normal group ($p < 0.05$). The CAT activity of both CPP and DMBG groups significantly increased compared with AD group ($p < 0.05$). GSH-px is assumed to be primarily

identified in the glial cytoplasm and to play a significant role in maintaining the blood–brain barrier and protecting the brain from oxidative stress (Price et al., 2006). The increased CAT helped remove H_2O_2 and reduce the metabolic burden on the brain (Rosemberg et al., 2010). Therefore, CPP appeared to effectively attenuate oxidative stress induced by STZ and D-gal.

3.4. Effect of CPP on the injury of tissues observed by histopathological examination

To further confirm a potential role of CPP in AD management, histopathological examination staining was employed to investigate histopathological changes in the liver, brain, jejunum, and pancreas. The cell architecture of the liver in normal group demonstrated the presence of a normal number of hepatocytes without shrinkage and collapse, normal intercellular space and nuclear, clear cell boundaries; however, in the AD group, cell degeneration and hypertrophy (black arrow), disordered arrangement, and vacuolization (black circle) were observed (Fig. 3a1-5) (Chen et al., 2019). Little to no significant changes were detected in the liver's physiological morphology between the CPPH and normal groups could be detected indicating that CPP reverted the hepatic damage induced from STZ. The brain tissues of normal mouse indicated that there were a range of neurons in a dense and neat pattern with round or oval nuclei, and the nucleoli in the cerebral microvessel were abundant and arranged in a clear and orderly manner without abnormalities (Fig. 3b1). However, some pathological features were often observed in injured brain, such as decrease in number of neurons, cellular arrangement disorders, and vacuolization (black circle), which could be observed in the AD group (Fig. 3b2) (Aydn et al., 2016; Metwally et al., 2018). After 4 weeks of intervention with DMBG and CPPH, the brain histopathological damages of the mice were mitigated with normal appearance and increasing number of neurons (Fig. 3b3-5). The jejunum affected the digestion and absorption of glucose, and jejunum abnormalities are observed among diabetic patients (Bikhazi et al., 2004). The jejunum tissue from normal group showed that the jejunum

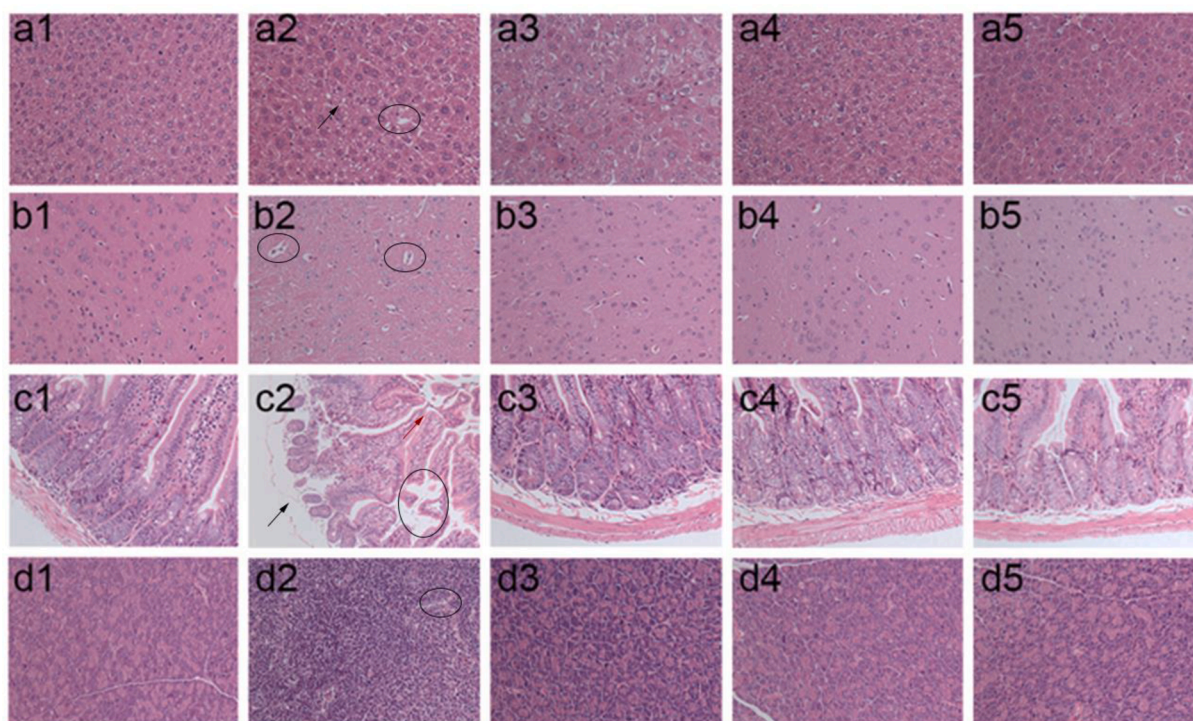


Fig. 3. CPP treatment improved histological appearance of (a) liver, (b) brain, (c) jejunum, and (d) pancreas of experimental mice (200 \times), including (1) normal, (2) AD, (3) DMBG, (4) CPPL, and (5) CPPH, respectively.

villi were neatly arranged with a complete and clear structure (Fig. 3c1). In contrast, jejunum tissues in AD group showed no integrity of the jejunum colon wall (black arrow) and the disordered arrangement of jejunum villi (red arrow) and vacuolization (black circle) could be observed (Fig. 3c2). The extent of these injuries was consistent with previous reports (Bikhazi et al., 2004). DMBG, CPPL, and CPPH administration restored this phenomenon and increased the length of jejunum villi (Fig. 3c3-5). The pancreatic tissue also showed significant improvement after CPP administration. The section of tissue in normal mice showed a normal histological structure with integral islet cells; however, a disorderly contraction of islet cells and gap increases (black circle) was observed in the AD group, and in accordance with reported negative effect of STZ (Fig. 3d1 & 3d2) (Rathinam et al., 2014). Compared with AD group, the islet cells of mice in both CPPL and CPPH groups were arranged in a tight and orderly manner and were similar to those in the normal group, which indicated that CPP had a certain repair effect on the pancreas after gavage (Fig. 3d3-5). Therefore, CPP had protective and repair effect on liver, brain, jejunum, and pancreas following STZ and D-gal induction.

3.5. Effects of CPP on glucose metabolism and aging-related gene expression of brain tissue in AD mice

To investigate whether CPP regulated the aging and glycol-metabolism in AD mice, RT-qPCR assay was performed to measure mRNA expression levels of pro-inflammatory cytokines and key metabolic enzymes in brain tissue. The aging factor P16 was determined, although there was no significant difference between the AD and normal groups, CPP reduced P16 expression despite no significant difference, whereas DMBG significantly decreased it compared with AD group ($p < 0.05$) (Fig. S1a). Therefore, a 45-mg/kg D-gal dose possibly induced aging, albeit not considerably severe (Liang et al., 2020; de Almeida-Rezende et al., 2021). FOXO-1 is regarded as potential target for aging and diabetes (Benchoula et al., 2021). The increased mRNA expression of FOXO-1 after induction appeared to decrease significantly after CPPL administration compared with that of AD group (Fig. 4c6) ($p < 0.05$). To determine the potential molecular targets, GLP-1R and IL-6R were investigated as therapeutic target for diabetes and aging, respectively, and were highly related to FOXO-1 (Wang et al., 2009; Kim et al., 2015).

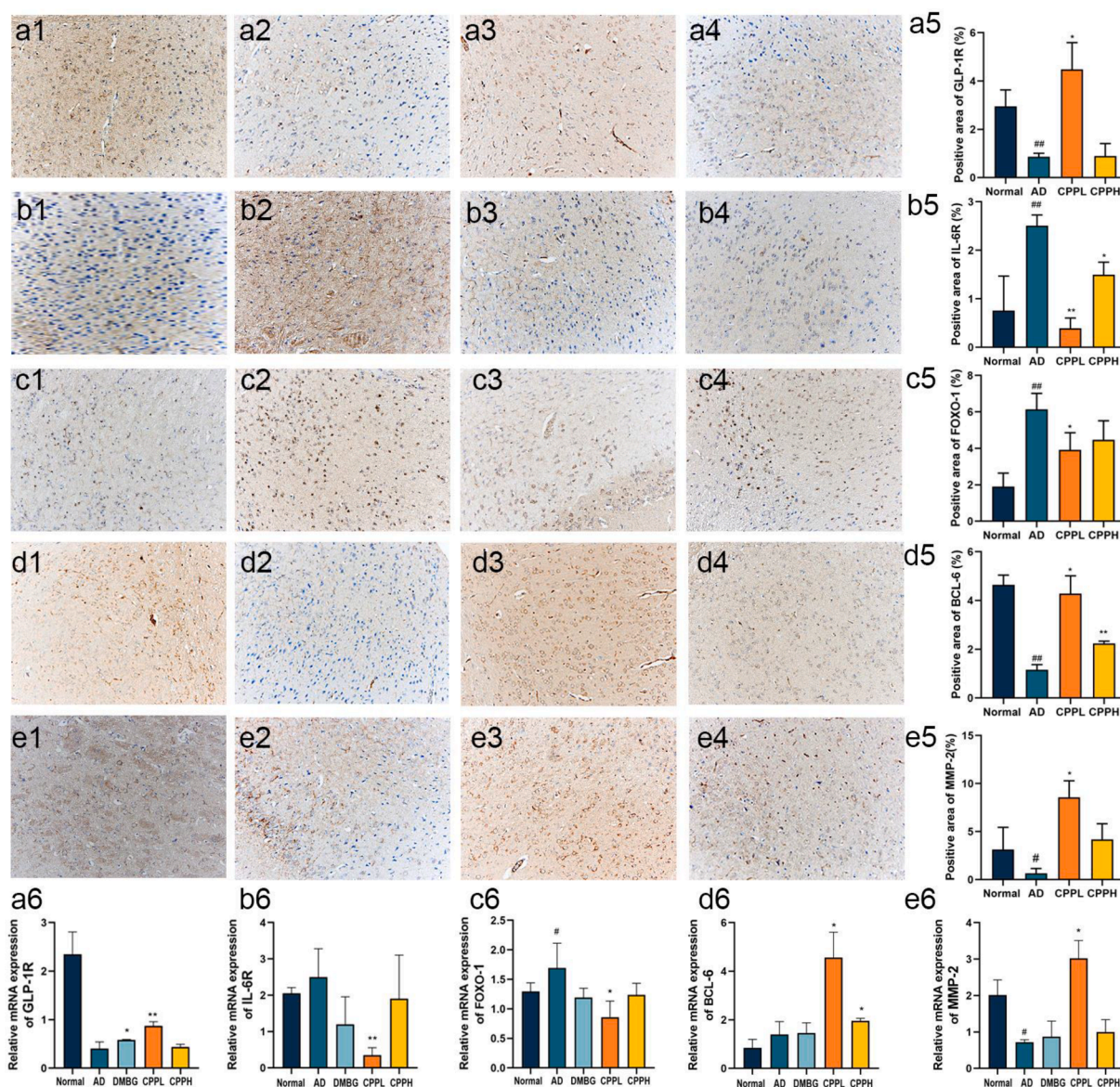


Fig. 4. Effect of CPP treatment on the relative protein expression of (a) GLP-1R, (b) IL-6R, (c) FOXO-1, (d) BCL-6, and (e) MMP-2 via IHC staining in (1) normal, (2) AD, (3) CPPL, and (4) CPPH group. The relative protein quantitative analysis is depicted in (5) whereas relative mRNA expression is presented in (6). Values represent the mean \pm SD ($n = 6$). * $p < 0.05$, ** $p < 0.01$ vs. AD mice; # $p < 0.05$, ## $p < 0.01$ vs. normal mice.

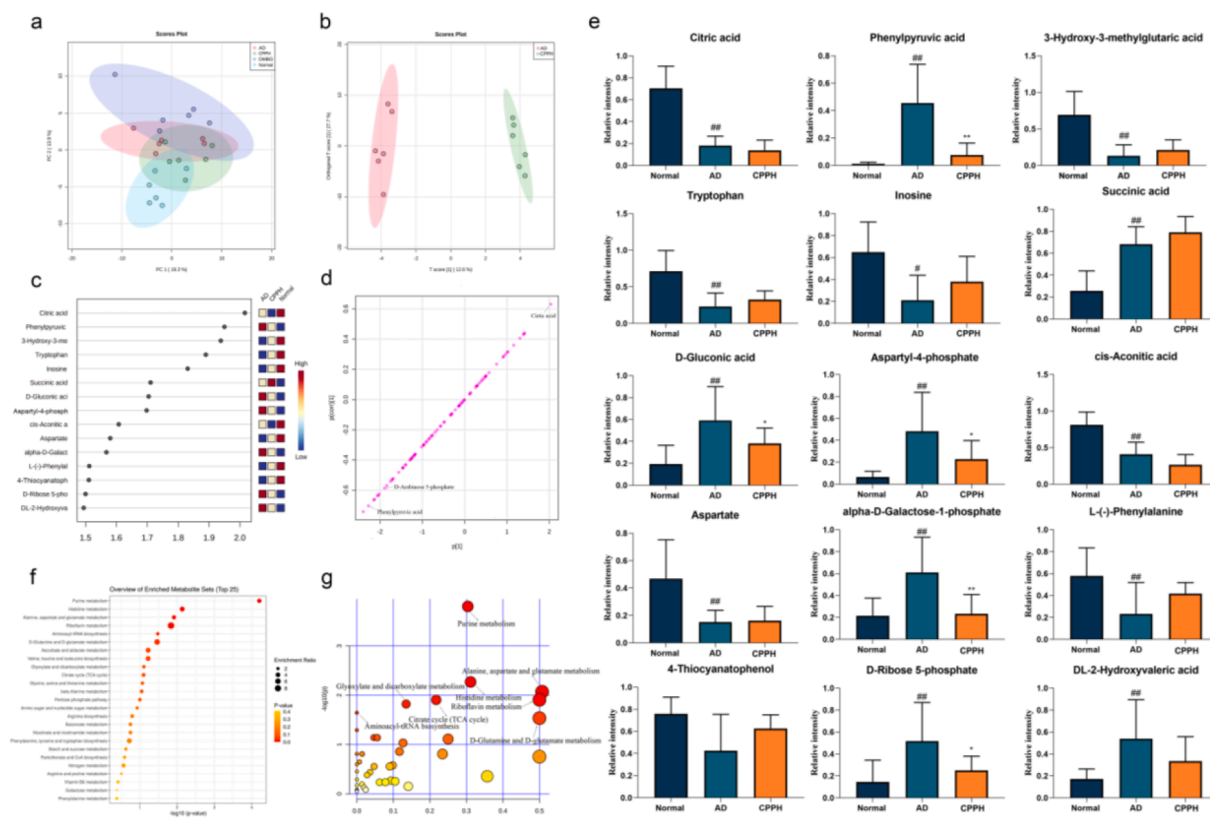


Fig. 5. CPHH treatment affected metabolites level in the brain tissue of diabetic mice. (a) PCA analysis, (b) OPLS-DA analysis, (c) VIP analysis, (d) S-plot and (e) barplots of the changes of crucial metabolites in mice brain as well as (f & g) enrichment analysis and pathway analysis of key metabolites. Data are the mean \pm SD ($n = 6$). * $p < 0.05$, ** $p < 0.01$ vs. AD mice ## $p < 0.01$ vs. normal mice.

The mRNA expression level of GLP-1R increased whereas that of IL-6R significantly decreased in the brain of AD group compared with that of normal group (Fig. 4a6 & 4b6) ($p < 0.05$). CPPL significantly improved these parameters when compared with the AD group ($p < 0.05$). The influence on MMP-2 and BCL-6 were further explored owing to the fact that they were downstream genes of FOXO-1 and to elucidate their effects on brain functions and role in preventing disease progression (Glaser and Schlegel, 2009; Huang and Li, 2014). Genes related to the blood–brain barrier, MMP-2, were measured and their expressions increased in the CPPL group compared with the AD group (Fig. 4e6) ($p < 0.05$). Similarly, a significant increase in BCL-6 level in the CPP group was observed compared with the AD group (Fig. 4d6) ($p < 0.05$).

The brain plays a major role in the regulation of normally developing organisms. Brain damage leads to the activation of the hypothalamic glucose-regulating neural circuits, leading to an overall rise in blood glucose level (Metwally et al., 2018). Therefore, it is crucial to explore the therapeutic mechanism of natural substances for AD through monitoring changes in the expression levels of the brain genes. Impairment of the blood–brain barrier often occurs in older people with diabetes and blood–brain barrier-promoted glucose transportation (Prasad et al., 2014). The present study reported that CPP improved MMP-2, which showed that CPP maintained the number of neurons and normal glucose transport by repairing the blood–brain barrier. Changes in GLP-1R and IL-6R, two major receptors on the cell surface, can affect BCL-6 through FOXO-1 regulation, leading to the occurrence or inhibition of cell apoptosis and aging (Glaser and Schlegel, 2009). However, GLP-1R can phosphorylate FOXO-1, which in turn enhances the diversity and number of neurons thereby regulating glucose balance (Kim et al., 2015). CPPL treatment led to increase in GLP-1R in AD mice, activation of BCL-6, and decrease in IL-6R (Fig. 4a6 & 4b6 & 4d6) ($p < 0.01$). These results indicated that CPP might alleviate AD-associated

apoptosis and inflammation and promote glucose homeostasis.

3.6. Effects of CPP on glucose metabolism and aging-related protein expression in brain tissue of AD mice

To confirm results inferred from the mRNA expression levels, which suggested the protective effects of CPP in brain tissue, changes in aging and diabetes related protein was measured via IHC. The trends in protein expression were the same as that in mRNA. The expression of GLP-1R in AD mice was significantly lower than that in normal mice ($p < 0.01$) and CPPL, but not CPPH, restored the condition (Fig. 4a1-5) ($p < 0.05$). IL-6R expression level appears to elevate after AD induction ($p < 0.05$), whereas it reduces in CPPL and CPPH animal groups (Fig. 4b1-5) ($p < 0.05$). FOXO-1 was highly expressed in AD group (Fig. 4c2). CPPL significantly decreased the expression of FOXO-1 and increased BCL-6 ($p < 0.05$), compared with AD group (Figs. 4c1-5 & 4d1-5). BCL-6 expression also increased after treatment with CPPL ($p < 0.05$) and CPPH ($p < 0.01$). Furthermore, there was a decrease in the expression of MMP-2 in the brain of AD animal group, this was consequently restored after CPPL administration ($p < 0.05$) (Fig. 4e1-5). Altogether, the above results corroborated the results of mRNA expression analysis and elucidated that the co-modulation of IL-6R/FOXO-1 and GLP-1R/FOXO-1 might be the possible mechanisms underlying the protective effects of CPP. However, this situation was opposite to biochemical indices likely attributed to different dose regimens (Li et al., 2021).

3.7. Effects of CPP on brain metabolites identified using liquid chromatography-mass spectrometry (LC-MS)

LC-MS analysis was used to deeply understand the difference of metabolites between the AD and the CPPH groups. LC-MS derived 88

peaks abundance among different groups were visualized using bioinformatics tools such as principal component analysis as unsupervised modelling of LC-MS dataset. Furthermore, OPLS-DA, as a supervised multivariate data analysis model, and its associated VIP and S-plots were used to identify the difference between the model and treatment groups as well as to identify potential biomarkers. PCA, in which each dot represents a simple sample, showed overlap among all samples, except for the distant clustering of the normal group along PC2 in the negative side. However, it had a relatively low total variance coverage of 32% of PC1 and PC2 (Fig. 5a). Consequently, supervised OPLS-DA was used showing improved separation between AD and CPPH group (Fig. 5b). The important metabolite whose correlation was > 0.5 and VIP of > 1.5 included citric acid, phenylpyruvic acid, 3-hydroxy-3-methylglutaric acid, gluconic acid, aspartyl-4-phosphate, *cis*-aconitic acid, galactose-1-phosphate ribose 5-phosphate, and 2-hydroxyvaleric acid in the CPPH group was significantly lower than those in AD group. In contrast, 3-hydroxy-3-methylglutaric acid, tryptophan, inosine, succinic acid, aspartate, phenylalanine, and 4-thiocyanatophenol appeared to increase (Fig. 5c). The corresponding S-plot was used to identify the variables that were responsible for differentiating AD group from CPPH group; this was further verified using VIP results (Fig. 5d). To further explore the therapeutic effect of CPP, 15 potential biomarkers were selected for detailed ANOVA analysis. After normalization processing, despite the presence of a significant difference in the selected biomarkers between the AD and CPPH groups, only phenylpyruvic acid and galactose-1-phosphate significantly affected aging and glucose metabolism after CPP treatment (Fig. 5e) ($p < 0.01$). Phenylpyruvic acid is a metabolite of phenylalanine, which inhibited glucose-6-phosphate dehydrogenase and leads to neurological disease, whereas galactose-1-phosphate resulted in permanent nervous system dysfunction (Rosa et al., 2012). Phenylpyruvic acid is also regarded as neurotransmitter and epinephrine-like substance with antidepressant effect (Shen et al., 2021). Our results revealed that CPP could regulate the injury induced by STZ and D-gal through changes in phenylpyruvic acid and galactose-1-phosphate levels. Therefore, CPP may improve glucose homeostasis and aging by regulating phenylpyruvic acid and galactose-1-phosphate.

To explore the effect of CPP on the metabolic pathways in AD mice, Metaboanalyst 4.0 software was used. The size of the shape represents

the degree of enrichment using hypergeometric test method, whereas depth of the color represents the significance. Pathways and enrichment with a p -value of < 0.05 were regarded as the closest pathways (Fig. 5f & 5g) to include purine metabolism, D-glutamine/D-glutamate metabolism, nitrogen metabolism, arginine biosynthesis, sphingolipid metabolism, pyruvate metabolism, galactose metabolism, alanine/aspartate metabolism, with D-glutamine/D-glutamate metabolism reported to play an important role in the regulation of aging and diabetes (Andersen et al., 2017). Previous studies reported disorder of purine metabolism after STZ induction such dysregulation to affect lifespan (Liu et al., 2015; Lennicke et al., 2020). Among the potential metabolites mentioned above (Fig. 5e), D-ribose 5-phosphate and inosine appeared to be enriched in purine metabolism according to KEGG database. Furthermore, CPP non-significantly regulated the levels of these metabolites. These results indicate that purine metabolism played the most important role in the regulation of AD (Fig. 5g), and was targeted by CPP in improving aging and glucose metabolism in that model.

3.8. Correlation between aging-related diabetes index and metabolomics

In order to determine the potential connection between metabolomics and AD indicators, Spearman correlation analysis was performed on these indicators and metabolite markers that showed VIP scores above 1.5. The AD indicators in liver related to oxidation resistance were significantly positively correlated with *cis*-aconitic acid, citric acid, tryptophan, 3-hydroxy-3-methylglutaric acid, whereas phenylpyruvic acid was significantly negatively correlated with antioxidant enzymes in the liver and brain (Fig. 6) ($p < 0.05$). The important indicator of regulation of diabetes, OGTT showed a strong positive correlation with phenylpyruvic acid, succinic acid, and aspartyl-4-phosphate and negative correlation with 3-hydroxy-3-methylglutaric acid and citric acid ($p < 0.01$), whereas insulin content was negatively correlated with phenylpyruvic acid and galactose-1-phosphate ($p < 0.05$). In the brain, CAT and GSH-px were both negatively associated with phenylpyruvic acid ($p < 0.05$). Increase in phenylpyruvic acid level could lead to nerve injury and DNA damage in glial cells, as previously observed in Alzheimer's patients (Liu et al., 2021). In diabetic patients, the high level of phenylpyruvic acid was also observed owing to the

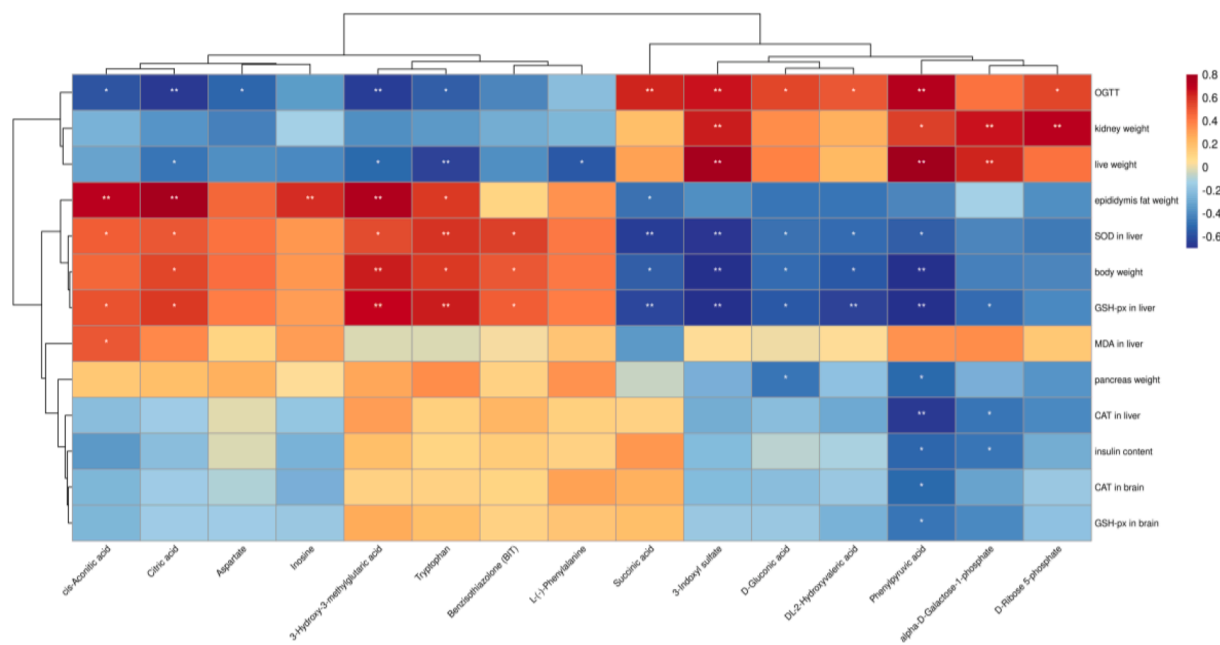


Fig. 6. Spearman's correlation analysis between potential marker metabolites and AD indices. Heatmap based on Spearman's correlation analysis. Color changed from blue for negative to red for positive correlations. (For interpretation of the references to color in this figure legend, the reader is referred to the web version of this article.)

impairment of phenylalanine metabolism (Men et al., 2017). Regarding weight change, body weight showed a negative correlation with phenylpyruvic acid, whereas the kidney weight was positively correlated with aspartyl-4-phosphate, phenylpyruvic acid, galactose-1-phosphate, and ribose 5-phosphate ($p < 0.05$) suggestive that brain metabolites play a potential role in weight regulation. Serotonin and metformin improved body and tissue weight by influencing appetite regulation (Lam et al., 2010; Malin and Kashyap, 2014). This result is consistent with changes in the aforementioned key metabolites in the brain of AD mice; in particular, it is likely that changes in phenylpyruvic acid level are related to AD regulation. Therefore, CPP could reduce oxidative stress and regulate insulin by decreasing the phenylpyruvic acid levels.

4. Conclusion

In summary, our findings suggested that CPP extracted from *C. pyrenoidosa* exerted a hypoglycemic activity and oxidation resistance in AD mice model. CPP inhibited high glucose-induced and aging-induced oxidative stress as well as inflammation through the upregulation of GLP-1R and downregulation of IL-6R, while maintaining blood–brain barrier homeostasis via the regulation of ZO-1 and MMP-2. CPP activated BCL-6 to promote cell survival in brain. Moreover, our metabolites profiling revealed that CPP has a positive effect by reducing phenylpyruvic acid and galactose-1-phosphate levels and by further influencing purine metabolism. Moreover, phenylpyruvic acid was the only metabolite that significantly regulated glucose metabolism and aging-related indices. Together, CPP might regulate AD by affecting phenylpyruvic acid levels to prevent oxidative stress and stimulate insulin. These findings highlight the potential of CPP in the prevention and intervention of aging T2D, a concept that has yet to be examined in other animal models or in humans in clinical settings.

Declaration of Competing Interest

The authors declare that they have no known competing financial interests or personal relationships that could have appeared to influence the work reported in this paper.

Acknowledgments

The project was funded by Key Project of the Natural Science Foundation of Fujian Province (2020J02032) and Fujian ‘Young Eagle Program’ Youth Top Talent Program.

Appendix A. Supplementary data

Supplementary data to this article can be found online at <https://doi.org/10.1016/j.fochx.2022.100316>.

References

- Agunloye, O. M., & Oboh, G. (2021). Blood glucose lowering and effect of oyster (*Pleurotus ostreatus*)-and shiitake (*Lentinus subnudus*)-supplemented diet on key enzymes linked diabetes and hypertension in streptozotocin-induced diabetic rats. *Food Frontiers*, 3(1), 161–171. <https://doi.org/10.1002/fft2.v3.110.1002/fft2.111>
- Andersen, J. V., Nissen, J. D., Christensen, S. K., Markussen, K. H., & Waagepetersen, H. S. (2017). Impaired hippocampal glutamate and glutamine metabolism in the *db/db* mouse model of type 2 diabetes mellitus. *Neural Plasticity*, 2017, 1–9. <https://doi.org/10.1155/2017/2107084>
- Atella, V., Piano Mortari, A., Kopinska, J., Belotti, F., Lapi, F., Cricelli, C., & Fontana, L. (2019). Trends in age-related disease burden and healthcare utilization. *Aging Cell*, 18(1), e12861. <https://doi.org/10.1111/acer.12861>
- Aydın, A. F., Çoban, J., Doğan-Ekici, I., Betül-Kalaz, E., Doğru-Abbasoğlu, S., & Uysal, M. (2016). Carnosine and taurine treatments diminished brain oxidative stress and apoptosis in D-galactose aging model. *Metabolic Brain Disease*, 31(2), 337–345. <https://doi.org/10.1007/s11011-015-9755-0>
- Benchoula, K., Arya, A., Parhar, I. S., & Hwa, W. E. (2021). FoxO1 signaling as a therapeutic target for type 2 diabetes and obesity. *European Journal of Pharmacology*, 891, 173758. <https://doi.org/10.1016/j.ejphar.2020.173758>

- Bikhazi, A. B., Skoury, M. M., Zwainy, D. S., Jurjus, A. R., Kreydiyyeh, S. I., Smith, D. E., ... Jacques, D. (2004). Effect of diabetes mellitus and insulin on the regulation of the PepT 1 symporter in rat jejunum. *Molecular Pharmacology*, 1(4), 300–308. <https://doi.org/10.1021/mp049972u>
- Bolli, G. B., Gottesman, I. S., Campbell, P. J., Haymond, M. W., Cryer, P. E., & Gerich, J. E. (1984). Glucose counterregulation and waning of insulin in the Somogyi phenomenon (posthypoglycemic hyperglycemia). *The New England Journal of Medicine*, 311(19), 1214–1219. <https://doi.org/10.1056/NEJM198411083111904>
- Chen, L., Fan, X., Lin, X., Qian, L., Zengin, G., Delmas, D., ... Xiao, J. (2019). Phenolic extract from *Sonchus oleraceus* L. protects diabetes-related liver injury in rats through TLR4/NF- κ B signaling pathway. *eFood*, 1(1), 77. <https://doi.org/10.2991/efood.k.191018.002>
- de Almeida Rezende, M. S., Oliveira de Almeida, A. J. P., Gonçalves, T. A. F., de Azevedo, F. d. L. A. A., Dantas, S. H., Silva, S. d. L., ... Bader, M. (2021). D-(+)-Galactose-induced aging: A novel experimental model of erectile dysfunction. *PLoS One*, 16(4), e0249487. <https://doi.org/10.1371/journal.pone.0249487>
- Fromenty, B., Vadrot, N., Massart, J., Turlin, B., Barri-Ova, N., Lettèron, P., ... Robin, M.-A. (2009). Chronic ethanol consumption lessens the gain of body weight, liver triglycerides, and diabetes in obese *ob/ob* mice. *Journal of Pharmacology and Experimental Therapeutics*, 331(1), 23–34. <https://doi.org/10.1124/jpet.109.155168>
- Fuster, J. J., Zuriaga, M. A., Zorita, V., MacLauchlan, S., Polackal, M. N., Viana-Huete, V., ... Walsh, K. (2020). TET2-loss-of-function-driven clonal hematopoiesis exacerbates experimental insulin resistance in aging and obesity. *Cell Report*, 33(4), 108326. <https://doi.org/10.1016/j.celrep.2020.108326>
- Giacco, F., & Brownlee, M. (2010). Oxidative stress and diabetic complications. *Circulation Research*, 107(9), 1058–1070. <https://doi.org/10.1161/CIRCRESAHA.110.223545>
- Glauser, D. A., & Schlegel, W. (2009). The FoxO/Bcl-6/cyclin D2 pathway mediates metabolic and growth factor stimulation of proliferation in Min6 pancreatic β -cells. *Journal of Receptors and Signal Transduction*, 29(6), 293–298. <https://doi.org/10.3109/10799890903241824>
- Huang, D.-W., Lo, Y. M., Chang, W.-C., Lin, C.-Y., Chen, J.-A., Wu, J.-B., ... Shen, S.-C. (2020). Alleviative effect of *Ruellia tuberosa* L. on NAFLD and hepatic lipid accumulation via modulating hepatic *de novo* lipogenesis in high-fat diet plus streptozotocin-induced diabetic rats. *Food Science and Nutrition*, 8(10), 5710–5716. <https://doi.org/10.1002/fsn3.v8.1010.1002/fsn3.1868>
- Huang, Y., & Li, L. P. (2014). Progress of cancer research on astrocyte elevated gene-1/Metadherin. *Oncology Letters*, 8(2), 493–501. <https://doi.org/10.3892/ol.2014.2231>
- Kazeem, M., Bankole, H., Ogunrinola, O., Wusu, A., & Kappo, A. (2021). Functional foods with dipeptidyl peptidase-4 inhibitory potential and management of type 2 diabetes: A review. *Food Frontiers*, 2(2), 153–162. <https://doi.org/10.1002/fft2.v2.210.1002/fft2.71>
- Kim, C. H. (2018). Microbiota or short-chain fatty acids: Which regulates diabetes? *Cellular and Molecular Immunology*, 15(2), 88–91. <https://doi.org/10.1038/cmi.2017.57>
- Kim, D. Y., Hwang, I., Muller, F. L., & Paik, J. H. (2015). Functional regulation of FoxO1 in neural stem cell differentiation. *Cell Death and Differentiation*, 22(12), 2034–2045. <https://doi.org/10.1038/cdd.2015.123>
- Lam, D. D., Garfield, A. S., Marston, O. J., Shaw, J., & Heisler, L. K. (2010). Brain serotonin system in the coordination of food intake and body weight. *Pharmacology Biochemistry and Behavior*, 97(1), 84–91. <https://doi.org/10.1016/j.pbb.2010.09.003>
- Lee, C. C., Sun, Y., & Huang, H. (2012). How type II diabetes-related islet amyloid polypeptide damages lipid bilayers. *Biophysical Journal*, 102(5), 1059–1068. <https://doi.org/10.1016/j.bpj.2012.01.039>
- Lennicke, C., dos Santos, E., & Cochemé, H. M. (2020). Sugar-induced dysregulation of purine metabolism impacts lifespan. *Aging (Albany NY)*, 12(24), 24479. <https://doi.org/10.18632/aging.104223>
- Li, Y., Wang, Y., Zhang, L., Yan, Z., Shen, J., Chang, Y., & Wang, J. (2021). α -Carrageenan tetrasaccharide from α -carrageenan inhibits islet β cell apoptosis via the upregulation of GLP-1 to inhibit the mitochondrial apoptosis pathway. *Journal of Agricultural and Food Chemistry*, 69(1), 212–222. <https://doi.org/10.1021/acs.jafc.0c06456>
- Liang, X., Yan, Z., Ma, W., Qian, Y.-i., Zou, X., Cui, Y., ... Meng, Y. (2020). Peroxiredoxin 4 protects against ovarian ageing by ameliorating D-galactose-induced oxidative damage in mice. *Cell Death Disease*, 11(12). <https://doi.org/10.1038/s41419-020-03253-8>
- Lin, H., Zhang, J., Li, S., Zheng, B., & Hu, J. (2021). Polysaccharides isolated from *Laminaria japonica* attenuates gestational diabetes mellitus by regulating the gut microbiota in mice. *Food Frontiers*, 2(2), 208–217. <https://doi.org/10.1002/fft2.v2.210.1002/fft2.79>
- Liu, J., Wang, C., Liu, F., Lu, Y., & Cheng, J. (2015). Metabonomics revealed xanthine oxidase-induced oxidative stress and inflammation in the pathogenesis of diabetic nephropathy. *Analytical and Bioanalytical Chemistry*, 407(9), 2569–2579. <https://doi.org/10.1007/s00216-015-8481-0>
- Liu, P., Yang, Q., Yu, N., Cao, Y., Wang, X., Wang, Z., ... Ma, C. (2021). Phenylalanine metabolism is dysregulated in human hippocampus with Alzheimer's disease related pathological changes. *Journal of Alzheimer's Disease*, 83(2), 609–622. <https://doi.org/10.3233/JAD-210461>
- Longo, M., Bellastella, G., Maiorino, M. I., Meier, J. J., Esposito, K., & Giugliano, D. (2019). Diabetes and aging: From treatment goals to pharmacologic therapy. *Frontiers in Endocrinology*, 10, 45. <https://doi.org/10.3389/fendo.2019.00045>
- Malin, S. K., & Kashyap, S. R. (2014). Effects of metformin on weight loss: Potential mechanisms. *Current Opinion in Endocrinology, Diabetes and Obesity*, 21(5), 323–329. <https://doi.org/10.1097/MED.0000000000000095>
- Men, L., Pi, Z., Zhou, Y., Liu, Y., Wei, M., Song, F., & Liu, Z. (2017). Metabolomics insights into diabetes nephropathy and protective effects of Radix Scutellariae on

- rats using ultra-high performance liquid chromatography coupled with quadrupole time-of-flight mass spectrometry. *RSC Advances*, 7(27), 16494–16504. <https://doi.org/10.1039/C6RA28595C>
- Metwally, M. M. M., Ebraheim, L. L. M., & Galal, A. A. A. (2018). Potential therapeutic role of melatonin on STZ-induced diabetic central neuropathy: A biochemical, histopathological, immunohistochemical and ultrastructural study. *Acta Histochemica*, 120(8), 828–836. <https://doi.org/10.1016/j.acthis.2018.09.008>
- Oboh, G., Oyeleye, S. I., Akintemi, O. A., & Olasehinde, T. A. (2018). Moringa oleifera supplemented diet modulates nootropic-related biomolecules in the brain of STZ-induced diabetic rats treated with acarbose. *Metabolic Brain Disease*, 33(2), 457–466. <https://doi.org/10.1007/s11011-018-0198-2>
- Ouyang, Y., Liu, D., Zhang, L., Li, X., Chen, X., & Zhao, C. (2022). Green alga *Enteromorpha prolifera* oligosaccharide ameliorates ageing and hyperglycemia through gut-brain axis in age-matched diabetic Mice. *Molecular Nutrition & Food Research*, 66(4), 2100564. <https://doi.org/10.1002/mnfr.v66.410.1002/mnfr.202100564>
- Prasad, S., Sajja, R. K., Naik, P., & Cucullo, L. (2014). Diabetes mellitus and blood-brain barrier dysfunction: An overview. *Journal of Pharmacovigilance*, 2(2), 125. <https://doi.org/10.4172/2329-6887.1000125>
- Price, T. O., Uras, F., Banks, W. A., & Ercal, N. (2006). A novel antioxidant N-acetylcysteine amide prevents gp120- and Tat-induced oxidative stress in brain endothelial cells. *Experimental Neurology*, 201(1), 193–202. <https://doi.org/10.1016/j.expneurol.2006.03.030>
- Rathinam, A., Pari, L., Chandramohan, R., & Sheikh, B. A. (2014). Histopathological findings of the pancreas, liver, and carbohydrate metabolizing enzymes in STZ-induced diabetic rats improved by administration of myrtenal. *Journal of Physiology and Biochemistry*, 70(4), 935–946. <https://doi.org/10.1007/s13105-014-0362-z>
- Rosa, A. P., Jacques, C. E., Moraes, T. B., Wannmacher, C. M., Dutra, A. M., & Dutra-Filho, C. S. (2012). Phenylpyruvic acid decreases glucose-6-phosphate dehydrogenase activity in rat brain. *Cellular and Molecular Neurobiology*, 32(7), 1113–1118. <https://doi.org/10.1007/s10571-012-9834-2>
- Rosemberg, D. B., da Rocha, R. F., Rico, E. P., Zanotto-Filho, A., Dias, R. D., Bogo, M. R., ... Souza, D. O. (2010). Taurine prevents enhancement of acetylcholinesterase activity induced by acute ethanol exposure and decreases the level of markers of oxidative stress in zebrafish brain. *Neuroscience*, 171(3), 683–692. <https://doi.org/10.1016/j.neuroscience.2010.09.030>
- Samaha, M. M., Said, E., & Salem, H. A. (2019). A comparative study of the role of crocin and sitagliptin in attenuation of STZ-induced diabetes mellitus and the associated inflammatory and apoptotic changes in pancreatic β -islets. *Environmental Toxicology and Pharmacology*, 72, 103238. <https://doi.org/10.1016/j.etap.2019.103238>
- Shen, D., Zhao, H., Gao, S., Li, Y., Cheng, Q. I., Bi, C., ... Yu, C. (2021). Clinical serum metabolomics study on fluoxetine hydrochloride for depression. *Neuroscience Letters*, 746, 135585. <https://doi.org/10.1016/j.neulet.2020.135585>
- Sivaraman, S. C., Vinnamala, S., & Jenkins, D. (2013). Gestational diabetes and future risk of diabetes. *Journal of Clinical Medicine Research*, 5(2), 92–96. <https://doi.org/10.4021/jocmr1201w>
- Suthagar, E., Soudamani, S., Yuvaraj, S., Ismail Khan, A., Aruldas, M. M., & Balasubramanian, K. (2009). Effects of streptozotocin (STZ)-induced diabetes and insulin replacement on rat ventral prostate. *Biomedicine and Pharmacotherapy*, 63(1), 43–50. <https://doi.org/10.1016/j.biopha.2008.01.002>
- Wan, X., Li, X., Liu, D., Gao, X., Chen, Y., Chen, Z., ... Zhao, C. (2021). Physicochemical characterization and antioxidant effects of green microalga *Chlorella pyrenoidosa* polysaccharide by regulation of microRNAs and gut microbiota in *Caenorhabditis elegans*. *International Journal of Biological Macromolecules*, 168, 152–162. <https://doi.org/10.1016/j.ijbiomac.2020.12.010>
- Wan, X.-Z., Ai, C., Chen, Y.-H., Gao, X.-X., Zhong, R.-T., Liu, B., ... Zhao, C. (2019). Physicochemical characterization of a polysaccharide from green microalga *Chlorella pyrenoidosa* and its hypolipidemic activity via gut microbiota regulation in rats. *International Journal of Biological Macromolecules*, 68(5), 1186–1197. <https://doi.org/10.1021/acs.jafc.9b06282>
- Wang, L., Yi, T., Kortylewski, M., Pardoll, D. M., Zeng, D., & Yu, H. (2009). IL-17 can promote tumor growth through an IL-6–Stat3 signaling pathway. *Journal of Experimental Medicine*, 206(7), 1457–1464. <https://doi.org/10.1084/jem.20090207>
- Wei, H., Li, L., Song, Q., Ai, H., Chu, J., & Li, W. (2005). Behavioural study of the D-galactose induced aging model in C57BL/6J mice. *Behavioural Brain Research*, 157(2), 245–251. <https://doi.org/10.1016/j.bbr.2004.07.003>
- Yuan, S., Yang, Y., Li, J., Tan, X., Cao, Y., Li, S., ... Zhang, Q. (2020). *Ganoderma lucidum* Rhodiola compound preparation prevent D-galactose-induced immune impairment and oxidative stress in aging rat model. *Scientific Reports*, 10(1). <https://doi.org/10.1038/s41598-020-76249-1>
- Zafar, M., & Hassan Naqvi, S. (2010). Effects of STZ-induced diabetes on the relative weights of kidney, liver and pancreas in albino rats: A comparative study. *International Journal of Morphology*, 28(1), 135–142. <https://doi.org/10.4067/S0717-95022010000100019>
- Zhao, C., Wan, X., Zhou, S., & Cao, H. (2020). Natural polyphenols: A potential therapeutic approach to hypoglycemia. *eFood*, 1(2), 107–118. <https://doi.org/10.2991/efood.k.200302.001>